Apoptosis
DOI 10.1007/s10495-017-1362-6

Changes in membrane lipids drive increased endocytosis following Fas ligation

Mauro Degli Esposti[1] · Paola Matarrese[2] · Antonella Tinari[2] · Agostina Longo[4] · Serena Recalchi[4] · Roya Khosravi-Far[3] · Walter Malorni[2] · Roberta Misasi[4] · Tina Garofalo[4] · Maurizio Sorice[4]

Abstract Once activated, some surface receptors promote membrane movements that open new portals of endocytosis, in part to facilitate the internalization of their activated complexes. The prototypic death receptor Fas (CD95/Apo1) promotes a wave of enhanced endocytosis that induces a transient intermixing of endosomes with mitochondria in cells that require mitochondria to amplify death signaling. This initiates a global alteration in membrane traffic that originates from changes in key membrane lipids occurring in the endoplasmic reticulum (ER). We have focused the current study on specific lipid changes occurring early after Fas ligation. We analyzed the interaction between endosomes and mitochondria in Jurkat T cells by nanospray-Time-of-flight (ToF) Mass Spectrometry. Immediately after Fas ligation, we found a transient wave of lipid changes that drives a subpopulation of early endosomes to merge with mitochondria. The earliest event appears to be a decrease of phosphatidylcholine (PC), linked to a metabolic switch enhancing phosphatidylinositol (PI) and phosphoinositides, which are crucial for the formation of vacuolar membranes and endocytosis. Lipid changes occur independently of caspase activation and appear to be exacerbated by caspase inhibition. Conversely, inhibition or compensation of PC deficiency attenuates endocytosis, endosome-mitochondria mixing and the induction of cell death. Deficiency of receptor interacting protein, RIP, also limits the specific changes in membrane lipids that are induced by Fas activation, with parallel reduction of endocytosis. Thus, Fas activation rapidly changes the interconversion of PC and PI, which then drives enhanced endocytosis, thus likely propagating death signaling from the cell surface to mitochondria and other organelles.

Keywords Cell death · Membrane lipids · Endosomes · Mitochondria · Membrane traffic

Abbreviations

D609	Tricyclodecan-9-yl xanthogenate
Er-PC	Erucyl-phosphocholine
HPA	Helix pomatia agglutinin
IETD	Benzyloxycarbonyl-Ile-Glu-Thr-Asp-fluoromethylketone
IVM	Intensified video microscopy
MPP	Mitochondrial membrane potential
MS	Mass spectrometry
MTR	Mitotracker®
PC	Phosphatidylcholine
PI	Phosphatidylinositol
RB	Modified ringer buffer
TEM	Transmission electron microscopy
z-VAD	Benzyloxycarbonyl-Val-Ala-Asp-fluoromethylketone

Tina Garofalo and Maurizio Sorice have equally contributed to this work.

Electronic supplementary material The online version of this article (doi:10.1007/s10495-017-1362-6) contains supplementary material, which is available to authorized users.

✉ Maurizio Sorice
maurizio.sorice@uniroma1.it

[1] Italian Institute of Technology, Genoa, Italy

[2] Department of Drug Research and Evaluation, Istituto Superiore Sanita', Rome, Italy

[3] Department of Pathology, Harvard Medical School, Beth Israel Deaconess Medical Center, Boston, MA 02215, USA

[4] Department of Experimental Medicine, Sapienza University, Viale Regina Elena 324, 00161 Rome, Italy

Published online: 15 March 2017

Introduction

The program of cell death involves biochemical changes in diverse intracellular organelles, in particular mitochondria [1]. Mitochondria are centrally positioned in the intrinsic pathway as well as the extrinsic, death receptor-mediated pathway of apoptosis [2]. In the majority of mammalian cell, death receptors require mitochondrial factors to amplify the activation of caspases [3, 4]. In these cells, usually called type II, engagement of mitochondria lags behind the rapid assembly of the signaling complex produced by receptor ligation at the cell surface [3, 5, 6].

Mitochondria also form a nexus in emerging connections between death receptor signaling and caspase-independent forms of cell death [7, 8]. For example, cardiolipin, a membrane lipid specific to mitochondria [9], is altered following activation of death receptors in a process fundamentally independent of caspases [10–14]. Alteration of membrane lipids may facilitate the engagement of mitochondria, since cardiolipin is specifically targeted by the caspase-cleaved form of Bid. Bid is a ubiquitous pro-apoptotic protein of the Bcl-2 family that functions as the major cytosolic link between apical caspases and mitochondrial membranes [5, 7, 15]. How cardiolipin becomes involved in the pro-apoptotic action of Bid and other Bcl-2 proteins has remained unclear [15, 16], considering that cardiolipin is predominantly located within the inner mitochondrial membrane, whereas pro-apoptotic proteins act on the outer mitochondrial membrane [2].

One possibility to explain how mitochondrial membrane lipids partake to the pro-apoptotic process is that other membrane organelles become intermixed with mitochondria during death signaling [7]. The dynamic aspects of intracellular organelles form part of membrane traffic, which follows diverse portals of endocytosis [17]. Emerging evidence indicates that death receptors are rapidly internalised after ligation, involving endocytic processes common to other receptors [6, 18–20]. The complexes formed by activated death receptors maintain signaling after internalization, thus using the early traffic of endocytic vesicles as a vehicle for intracellular communication [19–21]. The role of endosomal vesicles in death receptor-mediated apoptosis has been well characterized in type I cells, which do not require mitochondrial amplification of the caspase cascade [18, 20]. However, it is unclear how endocytic changes are linked to the propagation of death signaling [20, 22]. Further evidence also suggests that endosomal traffic may contribute to the engagement of mitochondria and other intracellular organelles in type II cells [23, 24]. In this work we have explored the mechanism of endocytic changes associated with the activation of Fas, the prototypic death receptor. The endocytic cycle requires specific changes in membrane lipids, with transient accumulation of phosphatidylinositol-3-phosphate (PI3P)—the signature lipid of early endosomes and an essential component of the membranes of all vacuoles [25, 26]. We have thus focused our studies on specific lipid changes occurring early after Fas ligation. Following prior investigations [12, 23], we have studied the interaction between endosomes and mitochondria in type II cells that are physiologically sensitive to Fas-mediated cell death. Immediately after Fas ligation, we found a transient wave of lipid changes that drives a subpopulation of early endosomes to merge with mitochondria, initiating a global alteration of the membrane traffic that precedes and possibly expand the caspase cascade of cell destruction.

Materials and methods

Reagents

Fluorescent probes and assays were purchased from Molecular Probes/Invitrogen (Eugene, OR). Tricyclodecan-9-yl xanthogenate (D609) was from Biomol (Plymouth Meeting, PA) and benzyloxycarbonyl-Val-Ala-Asp-fluoromethylketone (z-VAD) from Alexis (San Diego, CA). Recombinant superFasL was purchased from Apotech (Lausanne, Switzerland). Other chemicals were from Sigma (St. Louis, MO), GibCo and Fisher (Loughborough, UK).

Cell culture

Jurkat T cells were cultured in RPMI 1640 medium (Sigma–Aldrich, Milan, Italy) containing 10% foetal calf serum (FCS) plus 100 units/ml penicillin, 10 mg/ml streptomycin, at 37 °C in humified 5% CO_2 atmosphere.

Treatments

Cells were treated with 0.25 μg/ml recombinant FasL (Apotech, Lausanne, Switzerland) for 30 min and 60 min at 37 °C, in the absence of serum and the levels of apoptosis were evaluated by bi-parametric flow cytometry analysis [27], using a FACScan instrument (Becton Dickinson, Franklin Lakes, NJ, USA). In parallel experiments, cells untreated or treated with 0.25 μg/ml recombinant FasL, were incubated with z-VAD (a pan-caspases inhibitor) or D609 (a polyvalent phospholipase inhibitor) for 1 h at 37 °C.

Cell-death assay

Quantification of apoptosis was performed by flow cytometry after double cell staining with fluorescein isothiocyanate (FITC)–conjugated annexin V and Trypan blue

(Sigma), which allows discrimination among early apoptotic, late apoptotic, and necrotic cells.

Mitochondrial membrane potential in living cells

The mitochondrial membrane potential (MMP) of controls and treated cells was studied by using 5–5′,6–6′-tetrachloro-1,1′,3,3′-tetraethylbenzimidazol-carbocyanine iodide probe (JC-1, Molecular Probes). In line with this method, living cells were stained with 10 µM of JC-1. Tetramethylrhodamine ester 1 µM (TMRM), (Molecular Probes, red fluorescence) was also used to confirm data obtained by JC-1 (not shown).

Analysis of cytochrome *c* release

For cytochrome *c* release assays, 1×10^6 cells were seeded in 6-well plates and after 24 h were treated with FasL, in the presence or absence of zVAD or D-609. Cells were then collected by centrifugation. After washing three times in PBS, cells were suspended in 250 µl of hypotonic buffer (2 mM $MgCl_2$, 10 mM KCl, 10 mM Tris–HCl, pH 7.6) supplemented with complete protease inhibitor mixture (Roche Applied Science), and incubated on ice for 10 min. Cells were homogenized with a Teflon homogenizer with B-type pestle and, after addition of an equal volume of mitochondria buffer (400 mM sucrose, 10 mM TES, 400 µM EGTA, pH 7.2), centrifuged twice for 10 min at 900×*g* at 4 °C. The supernatant was recovered and further centrifuged for 15 min at 17,000×*g* at 4 °C. The pellet fraction was considered to be the mitochondria, and the supernatant was the cytosol. Release of cytochrome *c* was assessed by using a specific ELISA kit (R&D Systems, Minneapolis, MN) and expressed as ng/ml.

TEM analysis

Jurkat cells, untreated or treated with 0.25 µg/ml recombinant FasL, were fixed in 2.5% cacodylate-buffered (0.2 M, pH 7.2) glutaraldehyde for 20 min at room temperature and post-fixed in 1% OsO_4 in cacodylate buffer for 1 h at room temperature and processed as stated elsewhere [27]. Serial ultrathin sections were collected on 200-mesh grids, counterstained with uranyl acetate and lead citrate, and then analysed with a Philips 208 electron microscope at 80 kV.

Organelle isolation

Isotonic subcellular fractionation was carried out essentially as previously described by Sorice et al. [12] and illustrated in Supplementary Material Fig. 1. In detail, 1.5×10^8 cells, untreated or treated with 0.25 µg/ml recombinant FasL for 30 and 60 min at 37 °C were homogenized in 1 ml of cold isolation buffer (0.25 M Mannitol, 1 mM EDTA, 10 mM K-Hepes, 0.2% BSA, pH 7.4) containing a cocktail of protease inhibitors (Sigma). After a brief centrifugation at 600×*g*, pellet and supernatant were combined, rehomogenized and centrifuged at 800×*g* for 10 min at 4 °C. The pellet was discarded and the supernatant was further centrifuged at 10,000×*g* for 10 min at 4 °C. The pellets kept as fraction P10, was suspended in assay buffer (0.12 M mannitol, 0.08 M KCl, 1 mM EDTA, 20 mM K-Hepes, pH 7.4), or recentrifuged to obtain mitochondria. The supernatants were centrifuged at 22,000×*g* for 50 min to separate light membranes (fraction P20) from the cytosol (fraction S20).

After centrifugation at 9000×*g* for 15 min at 4 °C, the pellet was resuspended in 0.5 ml of assay buffer, centrifuged at 10,000×*g* for 10 min, and then resuspended in 25 µl of assay buffer with protease inhibitors (Supplementary Fig. 1). The purity of mitochondria (P10) and ER-rich fraction (P20) were verified by specific markers using anti-TOMM20 (mouse, Abcam, Cambridge, MA) and anti-prolyl-4-hydroxylase subunit β (P4HB) (rabbit, Abcam) respectively. After evaluation of the protein concentration by Bradford Dye Reagent assay (Bio-Rad, Hercules, CA, USA), fractions were stored at −80 °C.

Immunoblotting

Cell lysates and subcellular samples were separated by SDS-polyacrylamide gel electrophoresis (SDS-PAGE). The proteins were electrophoretically transferred onto polyvinyldene difluoride (PVDF) membranes (Bio-Rad). Membranes were blocked with 5% defatted dried milk in Tris-buffered saline (TBS), containing 0.05% Tween 20 and probed with rabbit anti-early endosomal antigen 1 (EEA1) polyclonal antibody (R&D Systems Inc., Minneapolis, MN, USA), polyclonal antibody anti-VDAC/porin and anti-p115 (Santa Cruz Biotechnologies, CA, USA). Bound antibodies were visualized with horseradish peroxidase (HRP)-conjugated anti-rabbit IgG and immunoreactivity was assessed by chemiluminescence reaction, using the ECL Western detection system (Amersham Buckinghamshire, UK).

Quantitative analysis of immunoblot images was carried out using NIH Image 1.62 as software (Mac OS X, Apple Computer International).

Lipid extraction and analysis by MS

After isolation, membrane subcellular fractions were subjected to lipid extraction in methanol:chloroform 1:1, as described earlier [11]. Samples were further mixed with 0.5 ml of 0.15 M NaCl and the organic phase was separated by centrifugation, dried under nitrogen, dissolved in chloroform, and centrifuged to remove any insoluble material.

Lipid samples were analysed by nanospray-Time-of-flight (ToF) Mass Spectrometry (MS) using either a QSTAR® (Applied Biosystems, Toronto, Canada), LCT or Q-TOF Micro (Micromass, Manchester, UK) instrument, usually set in positive ion mode. The cleared lipid extracts were infused into the mass spectrometer using capillary voltage at 2.250 V and sample cone at 35 V. The MS and MS/MS data were acquired in continuum mode over the range of 100–2000 m/z; for MS/MS the range depended on the m/z of the precursor ion.

For semiquantitative evaluation of lipid peaks, we used a variety of internal reference lipid ions that maintained equivalent relationships within multiple spectra of the same sample. Some of these ions showed little variation between control and apoptotic samples. These reference ions included sphingomyelin at 703.4 m/z [43] and the dominant phosphatidylethanolamine species, palmitoyl, stearoyl-phosphatidylethanolamine, at 768.6 m/z [13].

Concentration of phospholipids was evaluated from the content of organic phosphate, also using malachite green using our own modification of the PLD assay. Three experiments were repeated in each investigation.

Organelle staining

For mitochondria or endosomes detection, cells were specifically stained either in solution [for IVM analysis, cf. 27] or after attachment to polylysine-coated coverslips [28] with Mitotracker red for 1 h at 37 °C. After incubation, cells were fixed with 4% paraformaldehyde in PBS (w/v in PBS) for 30 min at room temperature and then permeabilized with 0.5% Triton X-100 in PBS for 5 min at room temperature. Cells were stained with anti-EEA1 polyclonal antibodies for 1 h at 4 °C, followed by three washes in PBS and addition of Alexa Fluor 488-conjugated anti-rabbit for additional 30 min. See figure legends for further details of fluorescence microscopy imaging.

Analysis of the effects of Er-PC on phospholipids biosynthesis and on endocytosis

Cells were treated with 20 µM erucyl-phosphocholine (Er-PC) for 1 h at 37 °C. After washing, pellets were subjected to organelle isolation (P20 and P10 fractions) and then to lipid extraction for MS analysis as described above. Alternatively, cells were subjected to fluorescence-based assays. Briefly, endocytosis was evaluated following the fluorescence changes of FM1-43 [28, 29] in either a plate reader (Fluoroskan Ascent, Thermo, Basingstoke, UK) or a spectrofluorimeter (Perkin-Elmer LC50: excitation at 470 nm and emission at 565–580 nm), using 5×10^5 cells/ml in a modified Ringer buffer (RB, containing 145 mM NaCl, 4.5 mM KCl, 2 mM $MgCl_2$, 1 mM $CaCl_2$, 5 mM K-Hepes, pH 7.4, and 10 mM glucose) and 2–4 µM FM1-43. The activity of cathepsin L was measured using the substrate rhodamine110-FR-bisamide [30].

Receptor-interacting protein (RIP) antisense modified cell line

Mammalian expression vectors were constructed to express a RIP antisense RNA, according to Pimentel-Muinos [31].

Data analysis and statistics

For flow cytometry studies all samples were analyzed by a dual-laser FACScalibur cytometer equipped with a 488 argon laser and with a 635 red diode laser. At least 20.000 events/sample were acquired. Data were recorded and statistically analyzed with a Macintosh computer using CellQuestPro Software. Col-lected data analysis was carried out by using ANOVA 2-way test for repeated samples by using Graphpad Prism software corrected for multiple comparisons by the Bonferroni procedure. All the data reported in this paper were verified in at least three different experiments and reported as mean ± standard deviation (SD). Only P values of less than 0.01 were considered as significant.

Results

Morphological evidence of vacuole-mitochondrial contacts after Fas activation in Jurkat cells

We previously found morphological evidence indicating a global polarization of endocytic membranes toward the Golgi apparatus, after Fas stimulation in T lymphoma cells [32]. Following these results, we next looked for possible intracellular changes, i.e. intermixing of endosomes with mitochondria, induced by FasL treatment in Jurkat cells using TEM analysis. After 1 h of FasL treatment we noted differences in terms of organelle distribution (Fig. 1b), as compared to untreated control cells (Fig. 1a). In particular, several mitochondria appeared to be approaching by vacuoles of different shape and origin. In some cases vacuoles, deriving from cellular membrane, seem to move toward mitochondria as observable in Fig. 1b (arrow). In other cases vacuoles appear to be in close contact with

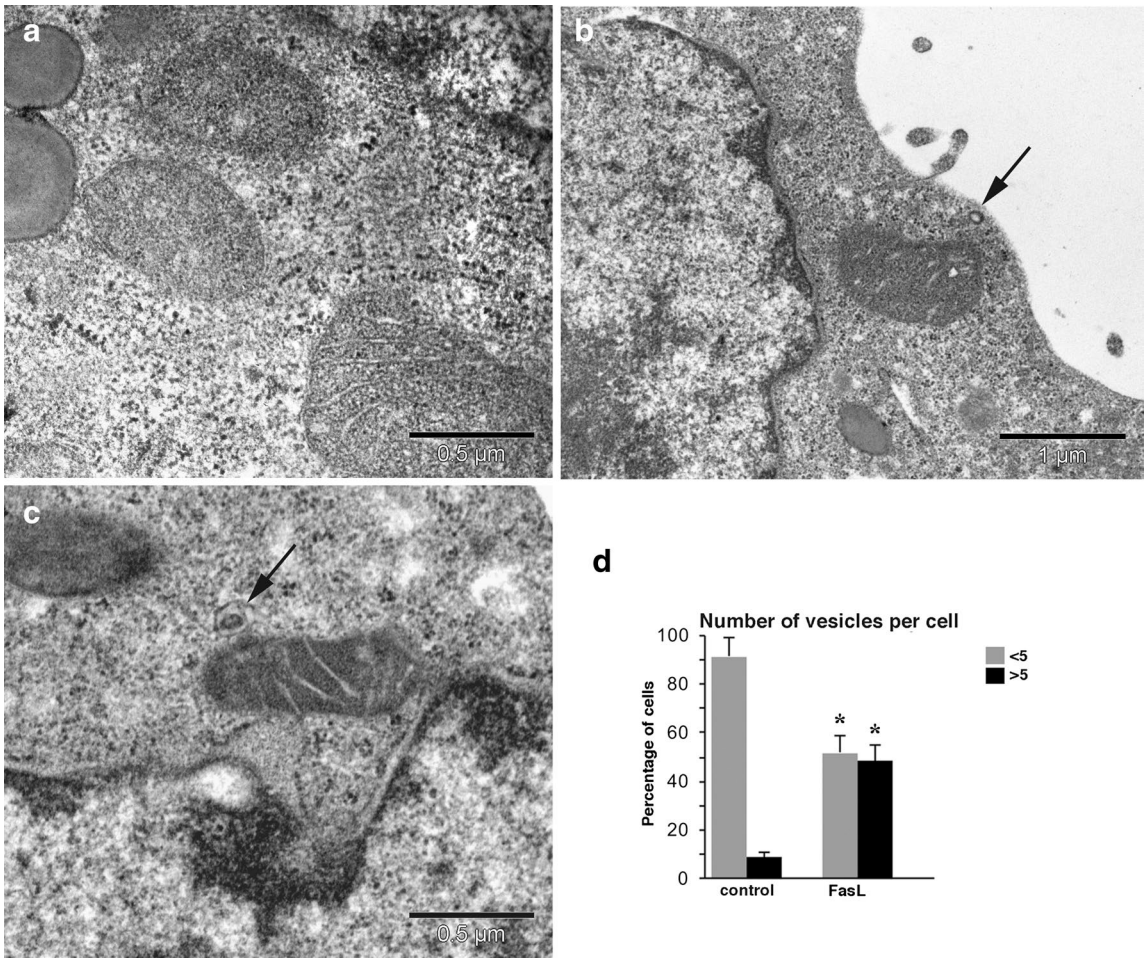

Fig. 1 Morphological evidence of endosome-mitochondria contacts after Fas activation TEM images of Jurkat cells untreated (**a**) or treated (**b, c**) with FasL. Ultrastructural analysis after FasL treatment revealed an increasing number of vacuoles as well as their increasing proximity to mitochondria. An untreated control cell is shown in (**a**). A vacuole migrating from cellular membrane toward mitochondria is displayed in (**b**, *arrow*), whereas a vacuole in close proximity to mitochondria is shown in (**c**, *arrow*). *Bars* 0.5 µm. **d** Morphometric analyses were performed by counting the number of vesicles in cell cytoplasm and evaluating the percentage of cells in which we observed some ($n < 5$, *grey columns*) or many ($n > 5$, *black columns*) vesicles. Three different grids for sample, for a total of at least 40 cells, were analyzed at the same magnification (×16,000). *$p < 0.01$ FasL-treated cells versus control cells

mitochondria (Fig. 1c, arrow). Of note, these cytological changes occurred before any morphological sign of apoptosis and resembled in part the vacuole fusion with mitochondria reported earlier in liver treated with TNFα [33].

Changes in membrane lipids induced by FasL

Starting from previously reported changes in phosphoinositides following PI3P elevation and from analysis on lipid extracts from Jurkat mitochondria containing abundant lipid metabolites related to PC [26, 34], we investigated the progressive alteration of membrane lipids during Fas signaling in Jurkat cells. After separating cell membranes with a subfractionation procedure [23], we found that FasL treatment (30 and 60 min) induced a significant change in the relative levels of long PC and PI species and their phosphorylated derivatives in ER-rich fraction P20 (Fig. 2a). Maximal increase of the PI species at 977 m/z (predominantly C40:6 Na3) and selected PIP species like those at 1005 and 1009 m/z (C38:2 Na3 and C40:6 Na2, respectively) occurred after 60 min of FasL treatment (Fig. 2a, arrow). Of note, the increase

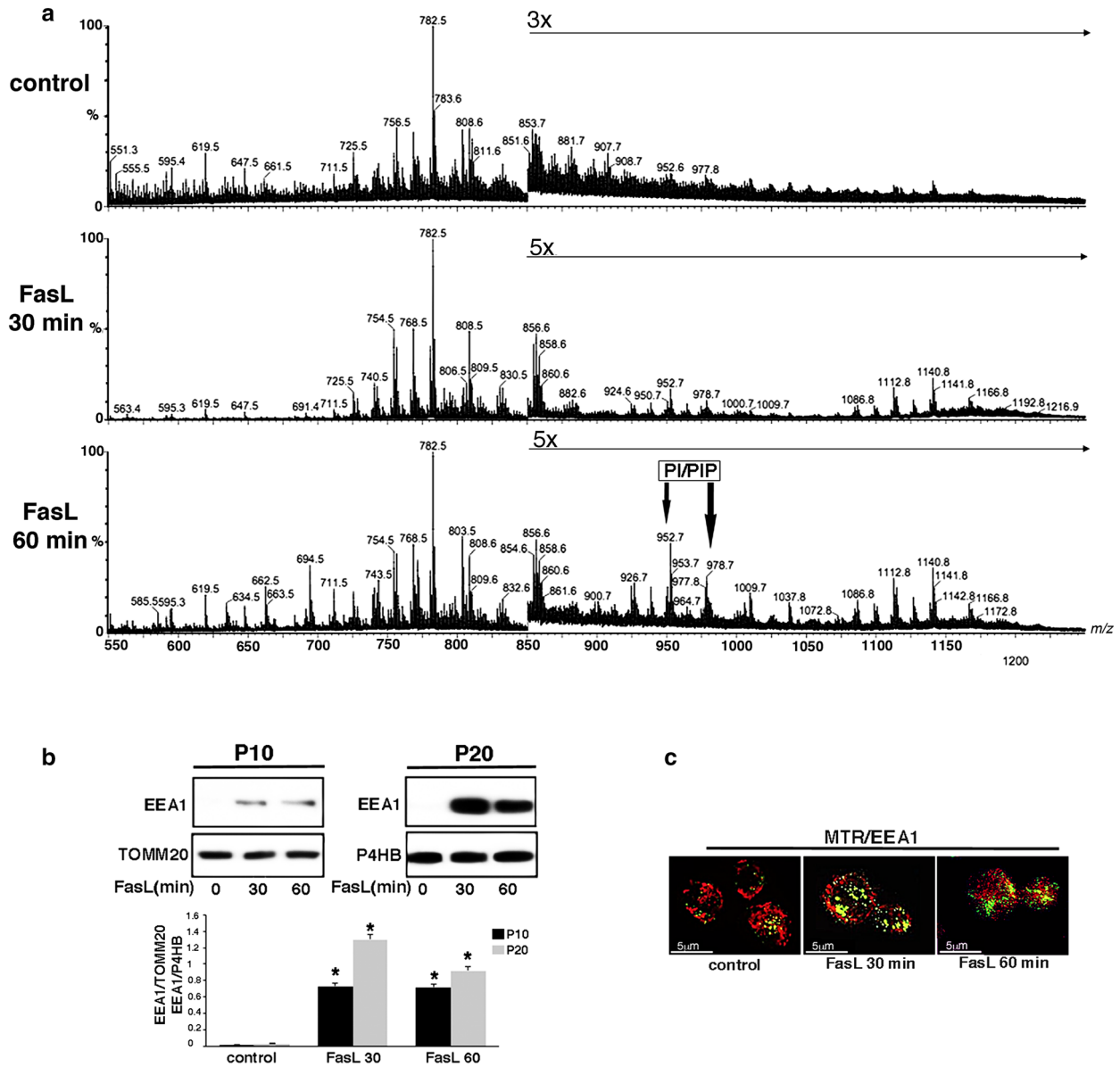

Fig. 2 Lipid changes and increase of early endosomes after FasL treatment. **a** MS profile of the lipid extracts from the P20 fraction of untreated (control) and FasL-treated Jurkat cells for 30 or 60 min. MS spectra of the PI/PIP region (>900 m/z) are amplified fivefold in treated cells; **b** detection of EEA1 in subcellular fractions of untreated or FasL-treated cells for 30 or 60 min. Mitochondria and P20 fraction were separated by SDS-PAGE and probed with anti-EEA1 at 4 °C overnight, using films (Fuji MI-NP 30) that allow enhanced quantitative resolution. Results obtained in a representative experiment are shown. Purity of subcellular preparations and loading control were evaluated by western blot, using antibodies versus mitochondrial marker TOMM20, and ER marker P4HB. Densitometric EEA1/TOMM20 ratios and EEA1/P4HB ratios are shown in the bottom panel. Results represent the mean ± SD from three independent experiments. $*p < 0.01$ FasL-treated cells versus control cells. **c** Overall projection of images from 56 z-sections obtained after 10 cycles of deconvolution by using a Deltavision RT system (Applied Precision) coupled to an automated Olympus IX71 microscope (×60 objective). Cells were first stained with 50 nM Mitotracker red (MTR), then attached to coverslips, fixed and permeabilised for EEA1 immunostaining, followed by Alexa Fluor488-conjugated anti-mouse. Note the increase in number and intensity of EEA1-positive vacuoles after FasL treatment (*central and right panel*). After 60 min-FasL treatment (*right panel*) mitochondrial fragmentation, typical of the execution phase of apoptosis, was observed

in these PI and PIP species closely matched the loss of SA-PC C38:4 (peaks at 810 and 832 m/z) and other long unsaturated phospholipids (Fig. 2a). These related changes appeared to be transient, consistent with the transient association of EEA1 to the membranes of the same fraction P20 (Fig. 2b). Indeed, a progressive increase of EEA1 was detected in the mitochondrial fraction of FasL treated cells (30 and 60 min, Fig. 2b). These results were also confirmed by densitometric analyses (Fig. 2b, bottom panel). Purity of subcellular preparations P10 and P20, were verified by TOMM20, a typical mitochondrial marker, and P4HB, an ER-associated protein marker, respectively. Immunofluorescence analysis confirmed this possibility, since after 30 min of FasL treatment there was a clear increase in the number and size of vacuoles positive for EEA1, some of which showed close spatial relations with mitochondria as indicated by discrete staining overlaps in deconvolution microscopy images. Virtually the same pattern was observed after 60 min of FasL treatment (Fig. 2c).

Pharmacological modulation of Fas-induced changes in membrane lipids

To verify the role of membrane lipids during Fas-mediated signaling, we analysed the whole spectrum of cellular membrane lipids after FasL treatment of Jurkat T cells, in the presence of either z-VAD to block all caspases (note that only caspase-8 was significantly activated under the conditions used [23]) and that has been shown to hinder apoptosis and MPP loss induced by FasL in human lymphoblastoid T-cell lines CEM [24] or D609, a polyvalent phospholipase inhibitor that has been previously shown to protect cells from Fas- and TRAIL-mediated cell death [13, 35] by modulating both endocytosis and cell death.

Within a comprehensive study of the membrane lipids of lymphoma cells, we concentrated on fraction P10 because it contained most cellular mitochondria but with variable levels of other organelles after FasL treatment. Significant depletion ($59 \pm 17\%$) of the major palmitoyl-oleoyl PC C34:1 was detected already after 30 min of FasL treatment, concomitantly with an average 50% loss of CL, as previously reported for TRAIL [13]. Block of caspases with z-VAD exacerbated the loss of PC induced by FasL and led to the accumulation of PC catabolites like oleate and diacylglycerol, DAG (fragment at 585 m/z, Fig. 3a). In essence, the profile of Fas-induced changes in membrane lipids indicated an overall imbalance between PC degradation and biosynthesis that was substantially reduced by D609 (Fig. 3a). The simplest possibility explaining this imbalance was that FasL treatment induced upstream inhibition of CTP:phosphocholine cytidylyltransferase (CCT), i.e. the critical enzyme of PC biosynthesis [36]. The MS profile of mitochondrial lipid extract from Jurkat control cells (without FasL) have already been shown in our previous papers [11, 14]. In particular, mitochondria from Jurkat cells, similar to those from most other cells, including mouse hepatocytes, contain a large complement of PC, which constitutes the dominant phospholipid of intracellular membranes. A by-product ion at 204 m/z (most probably the sodiated adduct of glyceryl-dimethylene-phosphate) appeared to be the most intense ion in the MS spectra obtained from the Q-TOF MS analysis.

Importantly, pre-treatment with D609 significantly reduced the depletion and remodeling of PC species that was induced by FasL (Fig. 3a). By considering the whole spectrum of major phospholipids and their metabolites, D609 attenuated the effects of Fas activation, producing changes of intermediate intensity with respect to those observed with FasL alone and FasL plus z-VAD. These related changes appeared to be transient, consistent with the transient association of EEA1 to the membranes of the same fraction P20. Of note, redistribution of EEA1 in P10 and P20 fractions induced by FasL occurred independently of caspase activation as evident in presence of z-VAD; in particular, caspase inhibition enhanced the association of EEA1 with mitochondria (Fig. 3b, right panel), as previously reported [23]. These results were also confirmed by densitometric analyses (Fig. 3b, bottom panel). Interestingly, Fas-mediated decrease of p115 in ER-rich membranes was observed (Fig. 3c), suggesting that p115 protein is dynamically associated with Golgi membranes and enhances the key enzymatic activity of PC metabolism, CCT, by direct binding to the enzyme [37].

Hence, the cumulative analysis of membrane lipids of FasL-treated Jurkat cells indicated an upstream alteration in the metabolic equilibrium between PC and PI initiated at the ER level. This alteration then reverberated onto mitochondrial membranes and could easily reflect an upstream inhibition of CCT, a possibility that was further reinforced by the Fas-mediated decrease of p115 in ER-rich membranes as showed by western blot analysis and confirmed by densitometric analyses (Fig. 3c).

As expected, cytofluorimetric analysis revealed a significant increase of apoptosis after FasL triggering with respect to untreated cells (Fig. 3d, bar graph in left panel and Supplementary Fig. 2, left column). According with this, the analysis of mitochondrial membrane potential, performed after cell staining with JC-1, showed a depolarization of mitochondrial membrane in a significant

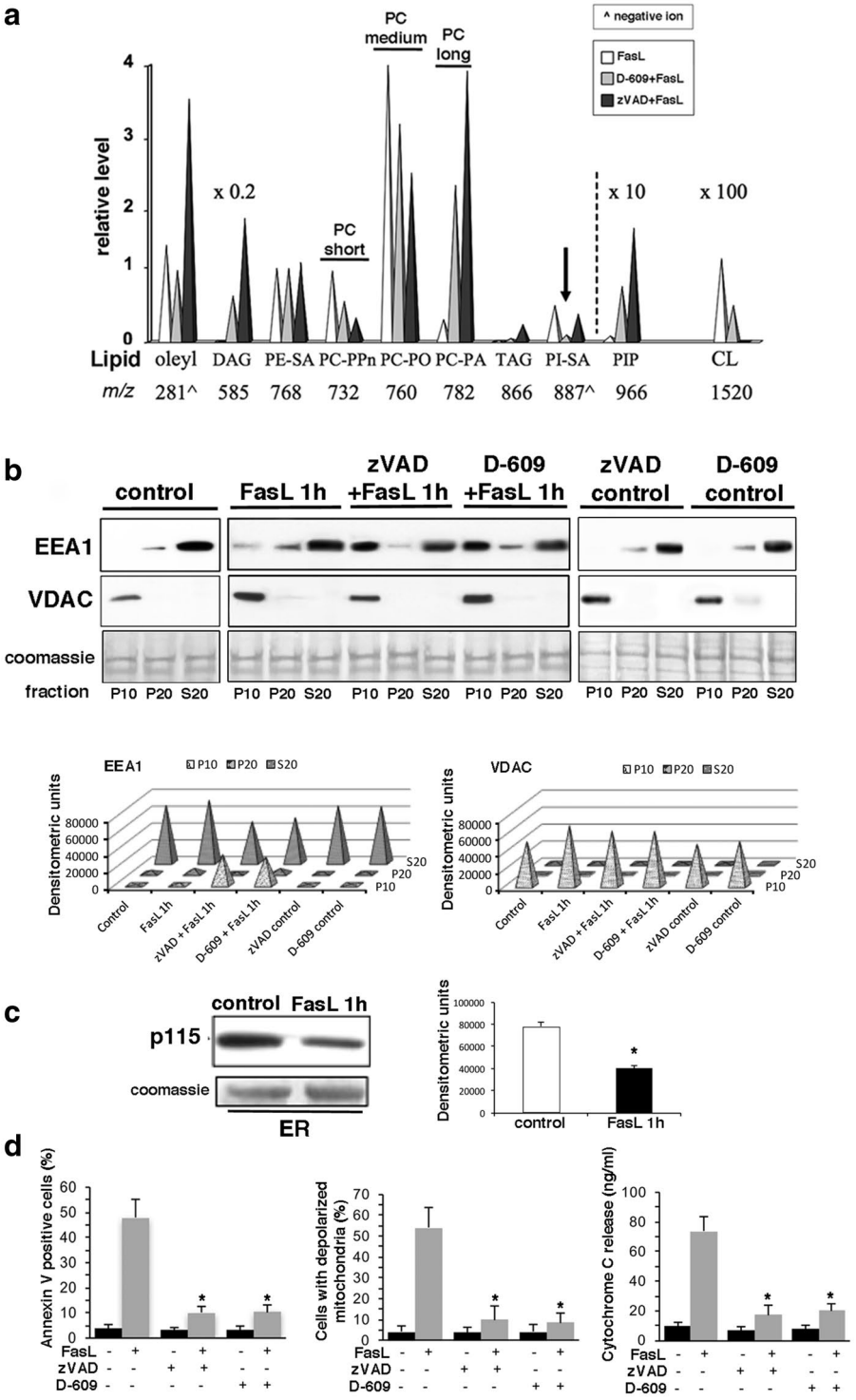

($p < 0.01$) percentage of FasL-triggered cells in comparison to control cells (Fig. 3d, bar graph in central panel and Supplementary Fig. 2, right column). In agreement with the biochemical data, cell pre-treatment with zVAD or D-609 was able to significantly prevent ($p < 0.01$) either apoptosis or mitochondrial membrane depolarization (Fig. 3d, bar

◂**Fig. 3** MS of lipids. **a** Semi-quantitative analysis of electrospray MS spectra of mitochondrial lipid ions as obtained under conditions minimizing the contribution of sodiated species (P10 fraction, i.e. unwashed mitochondria). The spectral data are represented as relative levels normalized to the intensity of the major PE species, 768 m/z, an internal reference ion displaying little changes during early apoptosis [13]. Computed values are the mean of 2–4 measurements and are reduced (DAG) or amplified (PIP and CL) to be comprised in the same scale. Note the FasL-induced depletion of short chain and medium PC species, the loss of major CL species (*right*) and the specific depletion of PI in the D609-treated sample (*arrow*). **b** *Upper panel* subcellular distribution of endosome markers. P10, P20 and S20 fractions obtained from untreated and FasL-treated cells in the absence or in the presence of z-VAD or D-609, were separated by SDS-PAGE and probed with anti-EEA1 or anti-VDAC/porin at 4 °C overnight. Results obtained in a representative experiment are shown. *Bar graph in the bottom panel* shows densitometric analysis in a representative experiment. Loading control was evaluated by coomassie blue staining. **c** Western blot analysis of p115 associated with equal loadings of untreated and FasL-treated cells in ER-enriched membranes (fraction P20). Results obtained in a representative experiment are shown. *Bar graph in the right panel* shows densitometric analysis. Results represent the mean ± SD from three independent experiments. $*p < 0.01$ FasL-treated cells *vs* control cells. **d** Bar graphs showing the analyses of apoptosis (*left panel*), MPP (*central panel*) and cytochrome *c* release (*right panel*). Values reported represent the percentage ± SD of data obtained from three different experiments. $*p < 0.01$ z-VAD or D-609 + FasL-treated cells versus FasL-treated cells

graph in left and central panels and Supplementary Fig. 2). Cell treatment with zVAD or D-609 alone did not induce any neither apoptosis nor mitochondrial membrane alteration (data not shown). These data were also corroborated by quantitative analysis of cytocrome *c* performed by ELISA, which highlighted as the release of cytochrome *c* induced by FasL was significantly inhibited by pre-treatment with zVAD or D-609 (Fig. 3d, bar graph in right panel).

Modelling of Fas-induced changes in membrane lipids: Er-PC treatment of Jurkat cells

Given the above indication for a Fas-induced dysregulation of PC-PI homeostasis, we next examined whether pharmacological inhibition of de novo biosynthesis of PC [38, 39] would reproduce the signature lipid changes observed in FasL-treated cells. T cells represent a good model to manipulate PC biosynthesis, since it is known that in these cells the expression of the alternative pathway of PE methylation is not effective [36]. Thus, we treated cells with cytotoxic concentrations of erucyl-phosphocholine (Er-PC) (Fig. 4). Er-PC is an anticancer alkyl-ether-lysophospholipid [40], that is closely related to edelphosine and equally depresses PC biosynthesis, primarily by inhibiting CCT [41, 42].

We first verified that Er-PC treatment enhanced endocytosis as described for similar compounds in other systems (Fig. 4a, left panel). Interestingly, Er-PC also enhanced the endocytic uptake of fluorescent dextran (Fig. 4a, right panel), as previously reported for genetic defects of CCT [39]. The membrane lipids of the same Er-PC-treated cells showed clear changes arising from strong inhibition of PC biosynthesis and metabolic alteration thereof, which appear to have altered the relative composition of major phospholipids (Fig. 4b). In particular, Er-PC induced an overall depletion of PC species accompanied by a large increase in the ion at 708 m/z, assigned to a byproduct of sodiated phosphatidic acid (PA)—a key precursor of PI [38]—and various sodiated, long PI species and related PIP species (Fig. 4b). Moreover, loss of long PC species was associated with the concomitant elevation in PI species having the same long unsaturated acyl chains (e.g. the decrease in C40:5 PC at 836 m/z in parallel to the increase of C40:5 PI-Na3 at 979 m/z). Consequently, acute inhibition of PC biosynthesis induced a metabolic shift from PC to long unsaturated PI species, including phosphatides instrumental to membrane traffic. We thus surmise that the enhanced membrane traffic due to the documented alteration in cellular membrane lipids may also affect the propagation of the apoptotic wave emanating from Fas receptor activation. Moreover, Er-PC-treated cells showed vacuoles in close proximity, or even merging with mitochondria, as revealed by TEM images (Fig. 4c, arrows in right panel), similarly to what observed in FasL treated cells.

RIP-deficiency attenuates lipid changes induced by FasL

Because pharmacological manipulation with D609 led to a complete inhibition of the global changes in membrane traffic that are elicited by Fas stimulation, and considering the broad spectrum of potential targets of D609, it was unclear which D609-sensitive step could be related to the earliest lipid changes driving endocytosis. Following previous findings showing a role of RIP in vacuole-dependent cell death [43], we decided to follow the genetic approach of down-regulating RIP expression to dissect key lipid changes and their effect on Fas-enhanced endocytosis.

We reasoned that if RIP were fundamental for modulating lipid interconnections, its genetic deficiency might produce recognizable changes in steady-state levels of PC, PI and CL even in resting cells. We thus examined the MS profile of all membrane lipids of Jurkat cells in which the dominant isoform of RIP was genetically ablated as showed

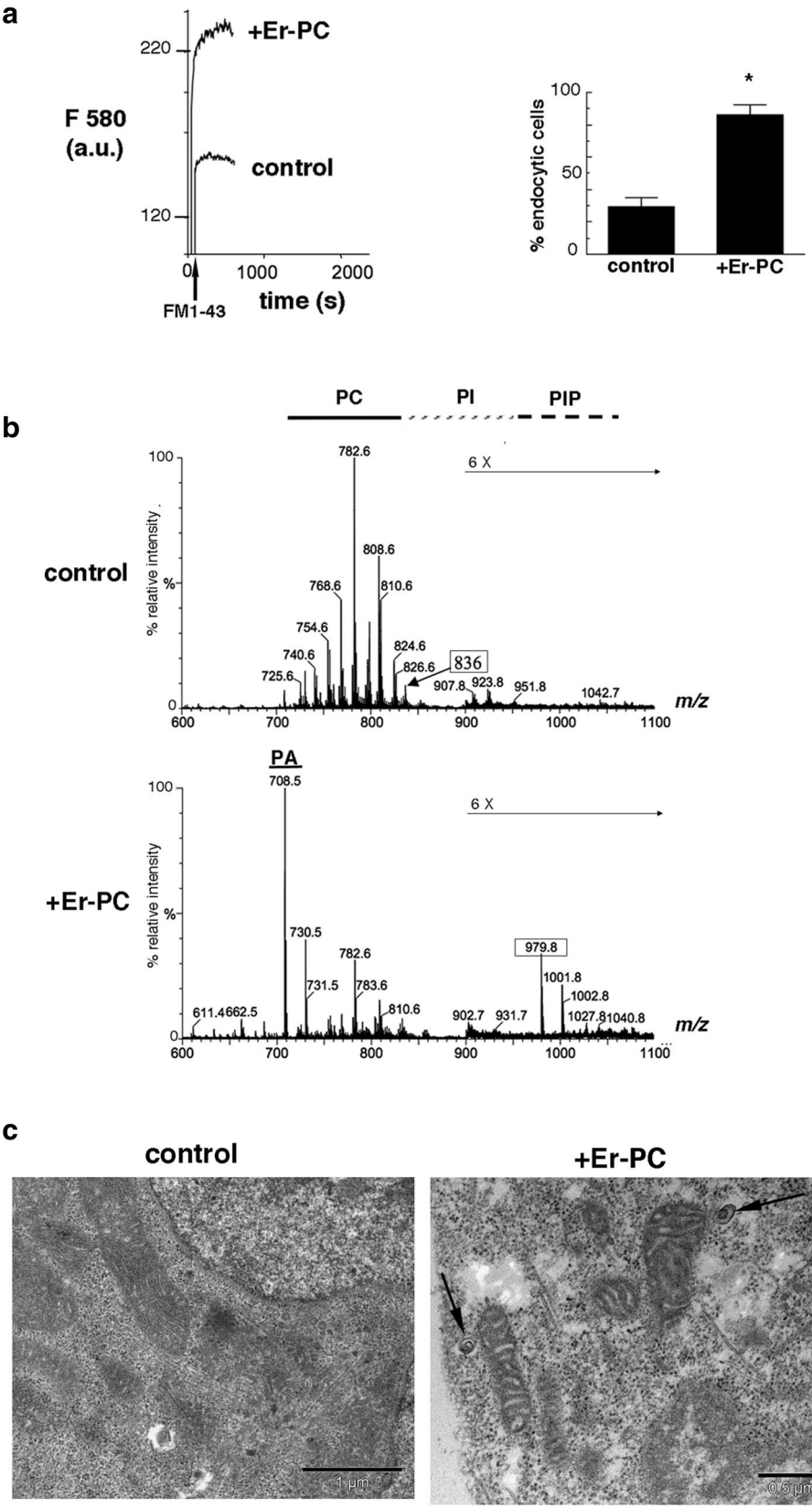
a
+Er-PC
control
F 580
(a.u.)
220
120
0
1000
2000
time (s)
FM1-43
% endocytic cells
100
50
0
control
+Er-PC
*
b
PC
PI
PIP
control
% relative intensity
782.6
6 X
808.6
768.6
810.6
754.6
824.6
740.6
826.6
836
725.6
907.8
923.8
951.8
1042.7
m/z
PA
+Er-PC
708.5
730.5
782.6
979.8
731.5
783.6
1001.8
1002.8
611.4662.5
810.6
902.7
931.7
1027.81040.8
c
control
+Er-PC
1 µm
0.5 µm

◂**Fig. 4** Modelling of membrane lipid changes in Jurkat cells with Er-PC. **a** The *left panel* shows on-line endocytosis of Jurkat cells incubated for 20 min after treatment with 20 μM Er-PC followed by a wash in full medium and re-suspension in Ringer buffer. The *right panel* shows flow cytometry evaluation of endocytosis in cells treated with 20 μM Er-PC for 1 h in the absence of serum. Results obtained in a representative experiment are shown. *Bar graph in the right panel* shows densitometric analysis. Results represent the mean ± SD from three independent experiments. $*p < 0.01$ Er-PC-treated cells versus control cells. **b** MS analysis of the lipid extract of total membranes (cumulative P20-P10 fractions) of the same cells as those used in (**a**). Note the depletion of PC and concomitant increase of long PI and various PI(3)P species, which are shown magnified sixfold in the right. **c** TEM image of Jurkat control cell (*left panel*) and treated cells with 20 μM Er-PC for 1 h showing the close contact between vacuoles and mitochondria (*right panel*)

by western blot analysis (Fig. 5a). In untreated cells, the absence of RIP enhanced the basal levels of the same short and medium PC species that were rapidly depleted following FasL treatment for 30 min Jurkat cells (Fig. 5b, c). It also modified the metabolic balance between PI and CL in favour of the latter (the dominant trioleoyl-arachidoyl-3Na CL at 1542 m/z increased by 50%), thus showing the opposite effect than treatment with FasL (Fig. 5c).

In complementary studies we observed that RIP-deficient cells exhibited no significant change in the caspase-stimulated dispersal of secretory endomembranes following the initial burst of endocytosis (Fig. 6). As shown in Fig. 6, the global changes in HPA-labelled membranes [dual HPA assay, cf. 23] that are normally induced by FasL treatment were affected by RIP deficiency. Indeed, RIP deficiency only affected surface and endocytic changes enhanced by FasL treatment which occurred beyond the levels observed in untreated cells (either wt or RIP-deficient).

Bypass of PC deficit rectifies early effects of FasL

To provide complementary evidence for the role of PC deficiency in the observed organelle scrambling, we tested whether exogenous lysophosphatidylcholine (LPC) could reduce phenotypic changes induced by FasL treatment (Fig. 7). It has been long established that defective PC biosynthesis (induced either genetically or pharmacologically) is effectively rectified by supplementing cells with exogenous LPC (Fig. 7a). This lysolipid is rapidly taken up and converted into intracellular PC, thereby bypassing the upstream block in PC production [36, 42, 44]. Exogenous LPC also protects from the apoptotic effects induced of PC deficiency [42, 44], as suggested here by quantitative evaluation of cell viability (Fig. 7b).

Discussion

We previously observed that the interaction of death receptor CD95/Fas with its physiological ligand, FasL, enhances endocytosis before the occurrence of apoptosis and independently of caspase activation in T cells [23, 24]. In particular, FasL binding is able to trigger a directional "movement" of some early and late endosomes towards mitochondria. We hypothesized that a sort of endosomal-stress can occur in the very early phases of receptor-mediated apoptosis in T cells. This may contribute to the complex organelle-crosstalk leading to the propagation of the signals to appropriate downstream effectors (e.g., to mitochondria) [45]. We show here that this propagation initiates a global alteration in membrane traffic that originates from changes in key membrane lipids occurring in the endoplasmic reticulum (ER). The earliest event appears to be a decrease of phosphatidylcholine (PC), linked to a metabolic switch enhancing phosphatidylinositol (PI) and phosphoinositides, which are crucial for the formation of vacuolar membranes and endocytosis. Lipid changes occur independently of caspase activation and appear to be exacerbated by caspase inhibition. Conversely, inhibition or compensation of PC deficiency attenuates endocytosis, endosome-mitochondria mixing and the induction of cell death.

In essence, the profile of Fas-induced changes in membrane lipids indicated an overall imbalance between PC degradation and biosynthesis that was substantially reduced by D609. The simplest possibility explaining this imbalance is that Fas activation induces upstream inhibition of CCT, i.e. the critical enzyme of PC biosynthesis [36]. Importantly, pre-treatment with the lipase inhibitor D609 significantly reduced the depletion and remodeling of PC species that was induced by FasL. Additional, yet unknown targets of DISC-activated enzymes could be involved in the global changes of membrane traffic we have documented here. On the basis of our results with D609, we hypothesize enzymes responsible for the rapid accumulation of PI and its phosphorylated forms are that among these targets. In type II cells that are physiologically sensitive to FasL-mediated death, DISC-activated enzymes may induce an early alteration of proteins that are critical for normal membrane traffic, thus promoting the transient dispersal of secretory organelles and their surface exposure.

For example, deficiency of receptor interacting protein (RIP) also attenuates the specific changes in membrane lipids that are induced by Fas activation, with parallel reduction of endocytosis. However, further studies are needed to confirm this observation.

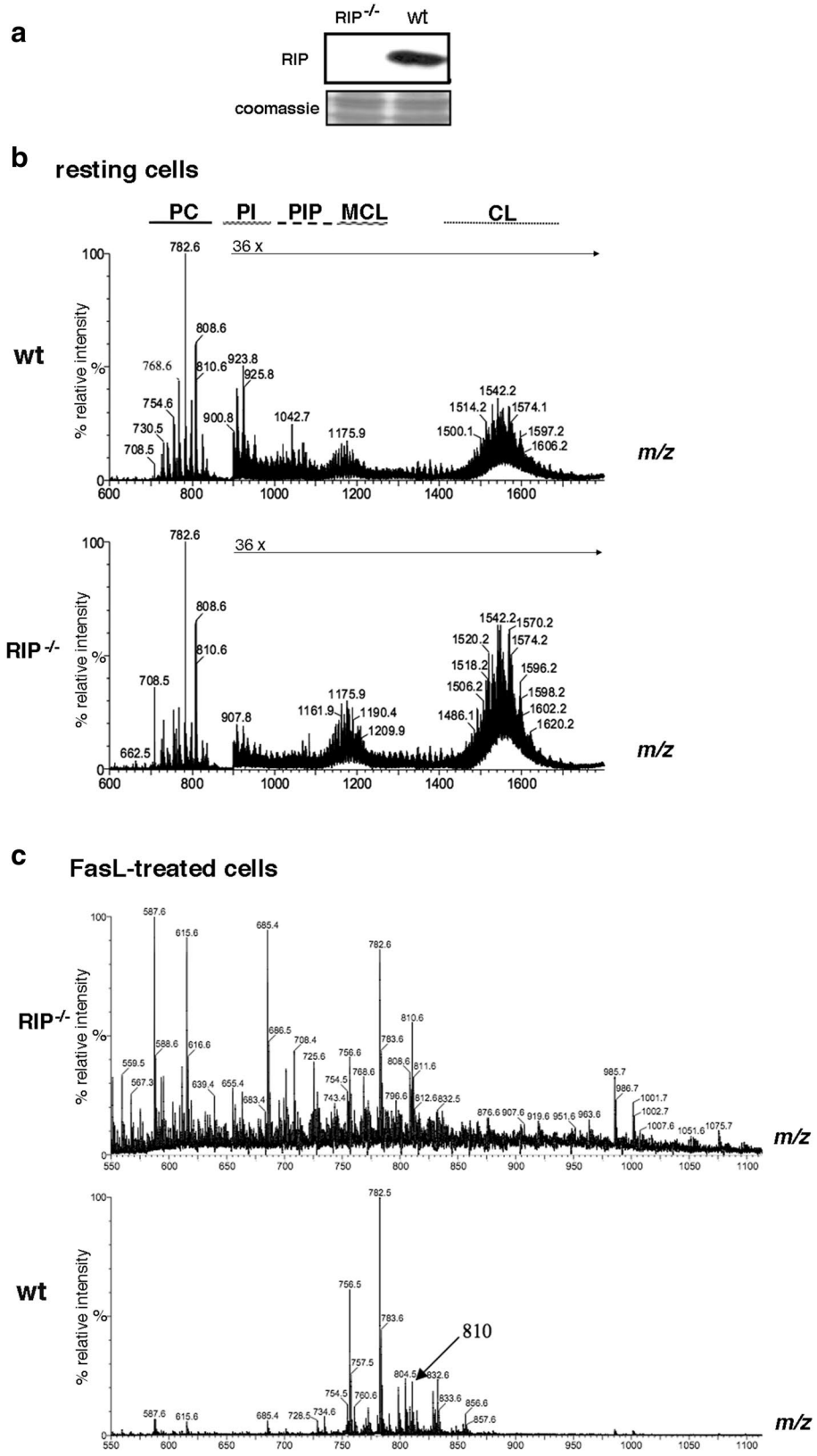

Fig. 5 MS analysis of mitochondrial membranes of RIP-deficient cells. **a** Western blot analysis of RIP in RIP-deficient ($RIP^{-/-}$) and the corresponding parental wild-type clone (wt) of Jurkat cells. Results obtained in a representative experiment from three independent experiments are shown. **b** MS analysis of membrane lipids (cumulative P20-P10 fractions) of parental wild-type and $RIP^{-/-}$ cells. The right part is magnified 36-fold. **c** MS profile of the membrane lipids extracted from fraction P20 from $RIP^{-/-}$ cells treated with FasL for 30 min (*top panel*). The *bottom panel* shows the reference MS profile of the lipids from the same fraction of wild type Jurkat cells. Note the increase in DAG species without loss of major PC species with concomitant increase in long PI species, contrary to what happens in wild-type cells treated with FasL

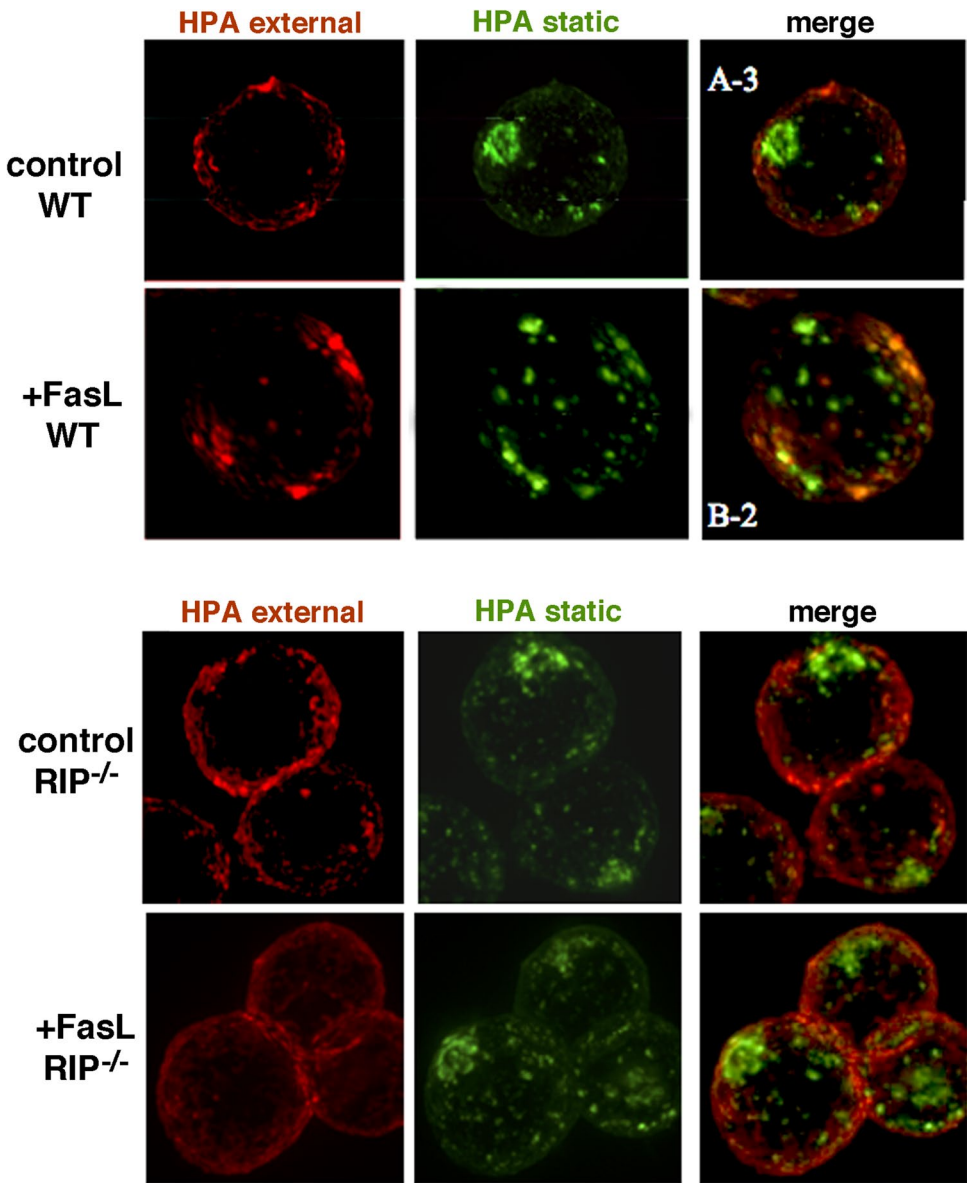

Fig. 6 Dual labelling of Golgi and endosomes and different effects of RIP deficiency and D609. Dual staining of mobile membrane elements was accomplished by incubating parental wild-type and RIP$^{-/-}$ cells with Texas-red-conjugated HPA (external, 20 mg/ml) simultaneously to FasL. Subsequent to fixation, cells were quenched with unlabelled HPA (52 mg/ml), permeabilized and then stained with Alexa Fluor 488-HPA (static HPA, 2 mg/ml for 5 min). After washing and mounting, images were obtained with Deltavision RT deconvolution microscopy

In conclusion, we suggest two fundamental phases in the complex changes of membrane traffic that are induced by Fas ligation:

1. a rapid rise in pinocytosis, propagating form the cell surface to its organelles including mitochondria, proceeding in a way which is caspase-independent but RIP-dependent;
2. a subsequent dispersal of intracellular organelles that is RIP independent but caspase-dependent.

Thus, Fas activation rapidly changes the interconversion of PC and PI, which then drives enhanced endocytosis, propagating death signalling from the cell surface to mitochondria and other organelles. This metabolic change is likely to be responsible for the movement of a subpopulation of early endosomes in proximity with mitochondria, contributing to the complex organelle-crosstalk that finally leads to cell demise [32, 45, 46].

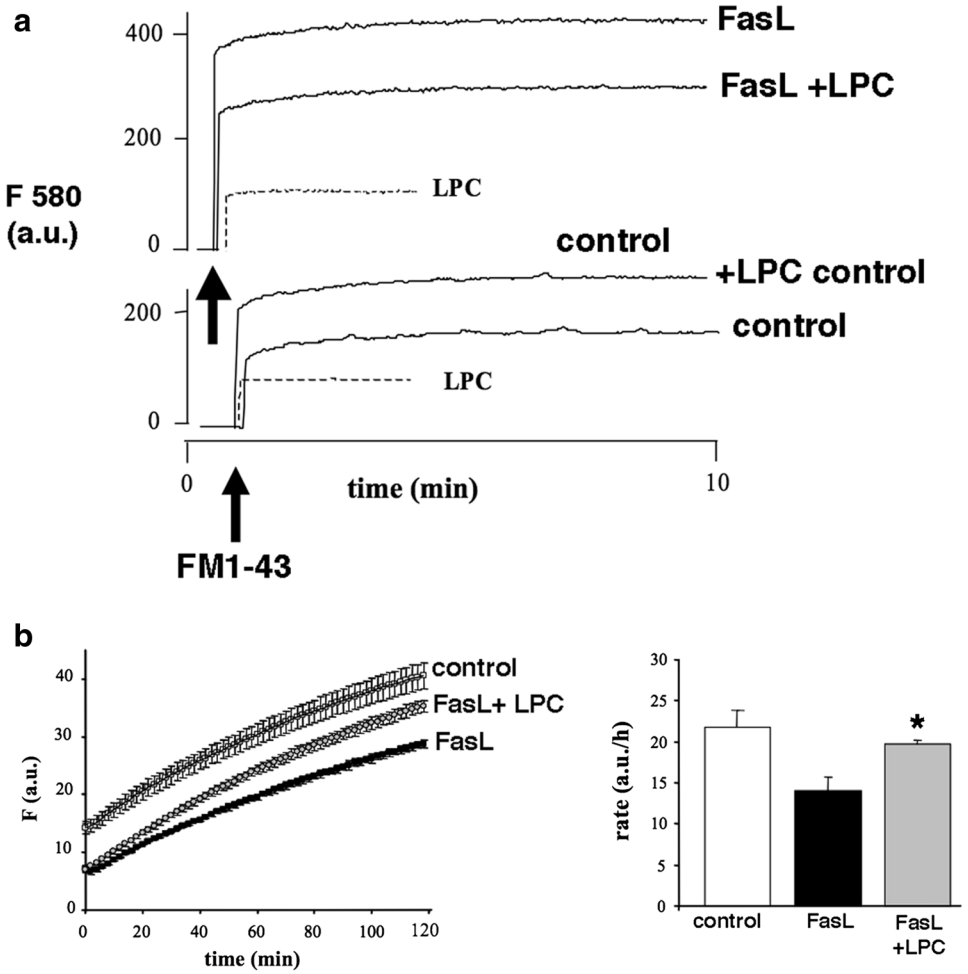

Fig. 7 Bypass of PC deficit reduces Fas-induced endocytosis and cell death. **a** Endocytosis assay in Jurkat cells using FM1-43 probe was undertaken after FasL administration for 30 min in the absence or presence of 10 μM LPC (a natural mixture from egg yolk) combined with BSA carrier (0.01%) to minimize membrane-damaging effects of the lysolipid. Note that FM1-43 fluorescence increased with the LPC/BSA mix (*dotted lines*) owing to incorporation in LPC micelles. **b** Cell viability was measured in a plate reader format (triplicate measurements), following resazurin fluorescence after incubation with FasL for 1 h. The starting point of the control time-course is offset upwards for sake of clarity. Results obtained in a representative experiment are shown. *Bar graph in the right panel* shows densitometric analysis. Results represent the mean ± SD from 3 independent experiments. $^*p < 0.05$ LPC/FasL-treated cells versus FasL-treated cells

References

1. Ferri KF, Kroemer G (2001) Organelle-specific initiation of cell death pathways. Nat Cell Biol 3:E255–E263
2. Chipuk JE, Green DR (2005) Do inducers of apoptosis trigger caspase-independent cell death? Nat Rev Mol Cell Biol 6:268–275
3. Scaffidi C, Fulda S, Srinivasan A, Friesen C, Li F, Tomaselli KJ, Debatin KM, Krammer PH, Peter ME (1998) Two CD95 (APO-1/Fas) signaling pathways. EMBO J 17:1675–1687
4. Peter ME, Krammer PH (2003) The CD95(APO-1/Fas) DISC and beyond. Cell Death Differ 10:26–35
5. Luo X, Budihardjo I, Zou H, Slaughter C, Wang X (1998) Bid, a Bcl2 interacting protein, mediates cytochrome *c* release from mitochondria in response to activation of cell death receptors. Cell 94:481–490
6. Garofalo T, Misasi R, Mattei V, Giammarioli AM, Malorni W, Pontieri GM, Pavan A, Sorice M (2003) Association of the death-inducing signaling complex with microdomains after triggering through CD95/Fas. Evidence for caspase-8-ganglioside interaction in T cells. J Biol Chem 278:8309–8315
7. Cristea IM, Degli Esposti M (2004) Membrane lipids and cell death: an overview. Chem Phys Lipids 129:133–160
8. Levine B, Yuan J (2005) Autophagy in cell death: an innocent convict? J Clin Invest 115:2679–2688
9. Schlame M, Greenberg ML (2017) Biosynthesis, remodeling and turnover of mitochondrial cardiolipin. Biochim Biophys Acta 1862:3–7
10. Matsko CM, Hunter OC, Rabinowich H, Lotze MT, Amoscato AA (2001) Mitochondrial lipids alterations during Fas- and radiation-induced apoptosis. Biochem Biophys Res Commun 287:1112–1120
11. Degli Esposti M, Cristea IM, Gaskell SJ, Nakao Y, Dive C (2003) Pro-apoptotic Bid binds to monolysocardiolipin, a new molecular connection between mitochondrial membranes and cell death. Cell Death Differ 10:1300–1309
12. Sorice M, Circella A, Cristea IM, Garofalo T, Di Renzo L, Alessandri C, Valesini G, Degli Esposti M (2004) Cardiolipin and its metabolites move from mitochondria to other cellular membranes during death receptor-mediated apoptosis. Cell Death Differ 11:1133–1145
13. Sandra F, Degli Esposti M, Magnus M, Knight D, Ndebele K, Khosravi-Far R (2005) TNF-Related Apoptosis Inducing Ligand (TRAIL) alters mitochondrial membrane lipids. Cancer Res 65:1–12
14. Goonesinghe A, Mundy E, Smith M, Khosravi-Far R, Martinou J-C, Degli Esposti M (2005) Pro-apoptotic Bid induces membrane perturbation by inserting selected lysolipids into the bilayer. Biochem J 387:109–118
15. Newmeyer DD, Ferguson-Miller S (2003) Mitochondria: releasing power for life and unleashing the machineries of death. Cell 112:481–490

16. Crimi M, Esposti MD (2011) Apoptosis-induced changes in mitochondrial lipids. Biochim Biophys Acta 1813:551–557
17. Conner SD, Schmid SL (2003) Regulated portals of entry into the cell. Nature 422:37–44
18. Algeciras-Schimnich A, Shen L, Barnhart BC, Murmann AE, Burkhardt JK, Peter ME (2002) Molecular ordering of the initial signaling events of CD95. Mol Cell Biol 22:207–220
19. Schneider-Brachert W, Tchikov V, Neumeyer J, Jakob M, Winoto-Morbach S, Held-Feindt J, Heinrich M, Merkel O, Ehrenschwender M, Adam D, Mentlein R, Kabelitz D, Schutze S (2004) Compartmentalization of TNF receptor 1 signaling: internalized TNF receptosomes as death signaling vesicles. Immunity 21:415–428
20. Lee KH, Feig C, Tchikov V, Schickel R, Hallas C, Schutze S, Peter ME, Chan AC (2006) The role of receptor internalization in CD95 signaling. EMBO J 25:1009–1023
21. Di Fiore PP, De Camilli P (2001) Endocytosis and signalling; an inseparable partnership. Cell 106:1–4
22. Austin CD, Lawrence DA, Peden AA, Varfolomeev EE, Totpal K, De Maziere AM, Klumperman J, Arnott D, Pham V, Scheller RH, Ashkenazi A (2006) Death-receptor activation halts clathrin-dependent endocytosis. Proc Natl Acad Sci USA 103:10283–10288
23. Ouasti S, Matarrese P, Paddon R, Khosravi-Far R, Sorice M, Tinari A, Malorni W, Degli Esposti M (2007) Death receptor ligation triggers membrane scrambling between Golgi and mitochondria. Cell Death Differ 14:453–461
24. Matarrese P, Manganelli V, Garofalo T, Tinari A, Gambardella L, Ndebele K, Khosravi-Far R, Sorice M, Degli Esposti M, Malorni W (2008) Endosomal compartment contributes to the propagation of CD95/Fas-mediated signals in type II cells. Biochem J 413:467–478
25. Simonsen A, Wurmser AE, Emr SD, Stenmark H (2001) The role of phosphoinositides in membrane transport. Curr Opin Cell Biol 13:485–492
26. Rink J, Ghigo E, Kalaidzidis Y, Zerial M (2005) Rab conversion as a mechanism of progression from early to late endosomes. Cell 122:735–749
27. Matarrese P, Tinari A, Mormone E, Bianco GA, Toscano MA, Ascione B, Rabinovich GA, Malorni W (2005) Galectin-1 sensitizes resting human T lymphocytes to Fas (CD95)-mediated cell death via mitochondrial hyperpolarization, budding, and fission. J Biol Chem 280:6969–6985
28. Dadsetan S, Shishkin V, Fomina AF (2005) Intracellular Ca2+ release triggers translocation of membrane marker fm1-43 from the extracellular leaflet of plasma membrane into endoplasmic reticulum in T lymphocytes. J Biol Chem 280:16377–16382
29. Kawasaki Y, Saito T, Shirota-Someya Y, Ikegami, Y Komano H, Lee, MH Froelich CJ, Shinohara N, Takayama H (2000) Cell death-associated translocation of plasma membrane components induced by CTL. J Immunol 164:4641–4648
30. Assfalg-Machleidt I, Rothe G, Klingel S, Banati R, Mangel WF, Valet G, Machleidt W (1992) Membrane permeable fluorogenic rhodamine substrates for selective determination of cathepsin L. Biol Chem Hoppe Seyler 373:433–440
31. Pimentel-Muinos FX, Seed B (1999) Regulated commitment of TNF receptor signaling: a molecular switch for death or activation. Immunity 11:783–793
32. Degli Esposti M, Tour J, Ouasti S, Ivanova S, Matarrese P, Malorni W, Khosravi-Far R (2009) Fas death receptor enhances endocytic membrane traffic converging into the Golgi region. Mol Biol Cell 20:600–615
33. Angermuller S, Kunstle G, Tiegs G (1998) Pre-apoptotic alterations in hepatocytes of TNFalpha-treated galactosamine-sensitized mice. J Histochem Cytochem 46:1175–1183
34. Lindmo K, Stenmark H (2006) Regulation of membrane traffic by phosphoinositide 3-kinases. J Cell Sci 119:605–614
35. Zhang L, Shimizu S, Tsujimoto Y (2005) Two distinct Fas-activated signaling pathways revealed by an antitumor drug D609. Oncogene 24:2954–2962
36. Cui Z, Houweling M (2002) Phosphatidylcholine and cell death. Biochim Biophys Acta 1585:87–96
37. Feldman DA, Weinhold PA (1998) Cytidylyltransferase-binding protein is identical to transcytosis-associated protein (TAP/p115) and enhances the lipid activation of cytidylyltransferase. J Biol Chem 273:102–109
38. Finney RE, Nudelman E, White T, Bursten S, Klein P, Leer LL, Wang N, Waggoner D, Singer JW, Lewis RA (2000) Pharmacological inhibition of phosphatidylcholine biosynthesis is associated with induction of phosphatidylinositol accumulation and cytolysis of neoplastic cell lines. Cancer Res 60:5204–5213
39. Weber U, Eroglu C, Mlodzik M (2003) Phospholipid membrane composition affects EGF receptor and Notch signalling through effects on endocytosis during Drosophila development. Dev Cell 5:559–570
40. Kugler W, Erdlenbruch B, Junemann A, Heinemann D, Eibl H, Lakomek M (2002) Erucylphosphocholine-induced apoptosis in glioma cells: involvement of death receptor signalling and caspase activation. J Neurochem 82:1160–1170
41. Baburina I, Jackowski S (1998) Apoptosis triggered by 1-O-octadecyl-2-O-methyl-rac-glycero-3-phosphocholine is prevented by increased expression of CTP:phosphocholine cytidylyltransferase. J Biol Chem 273:2169–2173
42. van der Luit AH, Budde M, Ruurs P, Verheij M, van Blitterswijk WJ (2002) Alkyl-lysophospholipid accumulates in lipid rafts and induces apoptosis via raft-dependent endocytosis and inhibition of phosphatidylcholine synthesis. J Biol Chem 277:39541–39547
43. Yu L, Alva A, Su H, Dutt P, Freundt E, Welsh S, Baehrecke EH, Lenardo MJ (2004) Regulation of an ATG7-beclin 1 program of autophagic cell death by caspase-8. Science 304:1500–1502
44. Boggs KP, Rock CO, Jackowski S (1995) Lysophosphatidylcholine attenuates the cytotoxic effects of the antineoplastic phospholipid 1-O-octadecyl-2-O-methyl-rac-glycero-3- phosphocholine. J Biol Chem 270:11612–11618
45. Tatsuta T, Langer T (2016) Intramitochondrial phospholipid trafficking. Biochim Biophys Acta. 10.1016/j.bbalip.2016.08.006
46. Milhas D, Andrieu-Abadie N, Levade T, Benoist H, Ségui B (2012) The tricyclodecan-9-yl-xanthogenate D609 triggers ceramide increase and enhances FasL-induced caspase-dependent and -independent cell death in T lymphocytes. Int J Mol Sci 13:8834–8852